







Research Article

Exploring the Effect and Mechanism of Si-Miao-Yong-An Decoction on Abdominal Aortic Aneurysm Based on Mice Experiment and Bioinformatics Analysis

Zhenyu Xu ¹, Lulu Zhang ², Ning Huangfu ¹, Fengchun Jiang ³, Kangting Ji ⁴,
and Shenghuang Wang ¹

¹Department of Cardiology, Ningbo First Hospital, Ningbo, Zhejiang, China

²Shanghai Medical College of Fudan University, Shanghai, China

³Department of Cardiology, Hangzhou Red Cross Hospital, Hangzhou, Zhejiang, China

⁴Department of Cardiology, Second Affiliated Hospital & Yuying Children's Hospital of Wenzhou Medical University, Wenzhou, Zhejiang, China

Correspondence should be addressed to Shenghuang Wang; 13605746913@163.com

Received 22 January 2022; Revised 26 April 2022; Accepted 19 May 2022; Published 31 May 2022

Academic Editor: Jian-You Guo

Copyright © 2022 Zhenyu Xu et al. This is an open access article distributed under the Creative Commons Attribution License, which permits unrestricted use, distribution, and reproduction in any medium, provided the original work is properly cited.

Background. Abdominal aortic aneurysm (AAA) is a fatal disease characterized by high morbidity and mortality in old population. Globally, effective drugs for AAA are still limited. Si-Miao-Yong-An decoction (SMYAD), a traditional Chinese medicine (TCM) formula with a high medical value, was reported to be successfully used in an old AAA patient. Thus, we reason that SMYAD may serve as a potential anti-AAA regime. **Objective.** The exact effects and detailed mechanisms of SMYAD on AAA were explored by using the experimental study and bioinformatics analysis. **Methods.** Firstly, C57BL/6N mice induced by Bap and Ang II were utilized to reproduce the AAA model, and the effects of SMYAD were systematically assessed according to histology, immunohistochemistry, and enzyme-linked immunosorbent assay (ELISA). Then, network pharmacology was applied to identify the biological processes, pathways, and hub targets of SMYAD against AAA; moreover, molecular docking was utilized to identify the binding ability and action targets. **Results.** In an animal experiment, SMYAD was found to effectively alleviate the degree of pathological expansion of abdominal aorta and reduce the incidence of Bap/Ang II-induced AAA, along with reducing the damage to elastic lamella, attenuating infiltration of macrophage, and lowering the circulating IL-6 level corresponding to the animal study, and network pharmacology revealed the detailed mechanisms of SMYAD on AAA that were related to pathways of inflammatory response, defense response, apoptotic, cell migration and adhesion, and reactive oxygen species metabolic process. Then, seven targets, IL-6, TNF, HSP90AA1, RELA, PTGS2, ESR1, and MMP9, were identified as hub targets of SMYAD against AAA. Furthermore, molecular docking verification revealed that the active compounds of SMYAD had good binding ability and clear binding site with core targets related to AAA formation. **Conclusion.** SMYAD can suppress AAA development through multicomponent, multitarget, and multipathway, which provides a research direction for further study.

1. Introduction

Abdominal aortic aneurysm (AAA) is a life-threatening vascular disease, mainly associated with the risk factors that include male gender, smoking, and old age [1]. AAA develops gradually and imperceptibly, and it is the tenth-leading killer of men older than 55 years in the United States [2]. In clinic, AAA is defined as a maximum abdominal

aortic diameter at least 1.5 times larger than the expected normal value [3]. For now, open or endovascular surgical repair is useless for most small AAA, and the specific medicine against AAA remains undeveloped [4]. Nowadays, AAA can be identified at early stage as a result of imaging and screening programs [5]. Thus, it is important to develop effective medical therapies that prevent the progressive expansion and rupture of AAA. For decades, large amount

of research studies were performed to increase the understanding of AAA pathogenesis and pathological features, including inflammation responses, oxidative stress, smooth muscle apoptosis, and extracellular matrix (ECM) degeneration [6–10]. Previous studies suggested that statins may have a potential effect on AAA [11, 12]. But in fact, statins' clinical effect is not satisfactory, and it has some side effects such as causing severe liver damage [13, 14]. Therefore, the focus should now be on searching new drugs with better efficacy and fewer side effects.

According to the dialectical treatment of TCM, AAA was primarily related to the blood stasis. Si-Miao-Yong-An decoction (SMYAD) is a traditional Chinese medicine (TCM) that has been used safely for hundreds of years. This classic ancient recipe was traditionally used for gangrene [15] and in the modern medicine therapy system to treat peripheral vascular diseases [16]. Among the four herbs included in SMYAD, *Flos Lonicerae* (Chinese name Jin-Yin-Hua), as the principal drug, has the efficacy of clearing away heat and detoxifying; *Radix Scrophulariae* (Chinese name Xuan-Shen) and *Radix Angelica Sinensis* (Chinese name Dang-Gui) are both adept in invigorating blood circulation and eliminating blood stasis; and *Radix Glycyrrhizae* (Chinese name Gan-Cao), as the mediator drug, coordinates the drug actions. Consequently, SMYAD can be used to promote poor blood circulation and remove detoxify, which means that it has the corresponding theoretical basis of TCM in the treatment of AAA. Moreover, SMYAD has been attempted to use in an old AAA patient and the clinic effect was fine [17]. However, the pharmacological effects, related pathways, and therapeutic core targets of SMYAD for treating AAA are still not well understood, which limit its wide use in clinical practice and further development.

Chinese materia medica is a complicated system of multicomponents, multitargets, and synergistic effect among compounds. Articulating the relationship among these elements is a difficult but fascinating challenge. Encouragingly, bioinformatics analysis provides us an up-to-date perspective to understand the interactions of compounds, pathways, and targets with disease [18]. It can also help us to efficiently screen potential drugs and comprehensively evaluate therapeutic mechanisms and targets of drugs on diseases. In this article, histology, immunohistochemistry, and enzyme-linked immunosorbent assay (ELISA) were used to evaluate the exact effects of SMYAD on 3, 4-benzopyrene (Bap)/angiotensin II (Ang II)-induced AAA mice. Then, bioinformatics analysis, including network pharmacology and molecular docking, was further utilized to perform visual analysis on the interaction of SMYAD and AAA, to identify the mechanisms, core targets, the potent compounds of SMYAD, and their targets in the treatment of AAA. The above all results suggested that SMYAD may be a potentially effective drug for AAA.

2. Materials and Methods

2.1. Experimental Animal. Male C57BL/6N mice, 6–7 months old, weighing 28–32 g were supplied by Charles River (Beijing, China) and maintained on a 12:12-hour light-

dark cycle with free ad libitum access to food and water for a one-week acclimatization period. Animal experiments were conducted in accordance with the guidelines for animal experiments of Wenzhou Medical University and approved by the animal ethics committee.

2.2. Preparation of SMYAD. Daily doses of SMYAD recorded in “*Yanfangxinpian*” (Qing dynasty) were *Flos Lonicerae* (90 g), *Radix Scrophulariae* (90 g), *Radix Angelica Sinensis* (60 g), and *Radix Glycyrrhizae* (30 g). The above-mentioned raw herbs were all obtained from Tongrentang pharmacy. According to the procedures of automatic decocting machine (HYDY-5), two copies of daily raw herbs (270 g × 2) were washed thoroughly and put into the decocting pot. The raw herbs were soaked in distilled water (1.5 L × 2) for 1 h and then decocted. Extracted solution (0.5 L × 2) was obtained after secondary filtered, and the concentration of the collected solution was equivalent to 0.54 g raw herbs/ml. The experimental dosage of SMYAD was determined according to the body surface conversion between human and mouse. Finally, the above solution was evaporated to the concentration of 13.2 g raw herbs/ml (defined as SMYAD-low dose) and 26.4 g raw herbs/ml (defined as SYMAD-high dose) by a rotary evaporator (LC-RE-5000). The above operations were repeated every day to prepare SMYAD.

2.3. Animal Grouping and Intervention. After one-week acclimatization, 42 mice were weighed and then randomly divided into two groups (count this day as Day 1): normal control group ($n = 6$, control for short) and model group ($n = 36$). From the Day 1 to Day 42, the 6 mice in control received no Bap/Ang II and other treatments; the 36 mice in the model group were injected intraperitoneally with Bap (B1760, Sigma-Aldrich) at a dose of 10 mg/kg body weight weekly and a dose (0.72 mg/kg/day) of Ang II (A9525, Sigma-Aldrich) using subcutaneous osmotic mini-pumps (Model# 2006, Alzet). Current guideline for use of bio-hazardous materials was followed when using Bap. At Day 15, 36 mice in the model group were randomly and equally divided into three groups, namely, Bap-/Ang II-treated + saline group (Bap + Ang II for short, $n = 12$), Bap-/Ang II-treated + SMYAD-low-dose group (Bap + Ang II + SL for short, $n = 12$), and Bap-/Ang II-treated + SMYAD-high-dose group (Bap + Ang II + SH for short, $n = 12$). From Day 15 to Day 42, mice in Bap + Ang II + SL and Bap + Ang II + SH were fed intragastrically 1 ml of SMYAD-low dose or SMYAD-high dose once daily, respectively; meanwhile, mice in Bap + Ang II were fed intragastrically with 1 ml of saline solution once daily. On Day 43, all survival mice were weighed and then euthanized.

2.4. Evaluation of Aortas and Histological Examination. After euthanasia, the thoracic and abdominal cavities were probed, and the aorta was sequentially irrigated with PBS and 4% formaldehyde through the left ventricle. Macroscopic examination of aortas was performed and carefully cleaned under a dissection microscope. The suprarenal

segments or obvious lesions of abdominal aorta were dissociated and fixed in 10% paraformaldehyde and then embedded in paraffin wax. The paraffin slices of the abdominal aortic sections (4 μm thick) were prepared and stained with haematoxylin-eosin (HE) stain. HE stain was used to assess the morphology and structure of abdominal aorta. Due to the irregular shapes of slices, the perimeter, instead of diameter, was measured with ImageJ for comparison. For each animal, two slices of abdominal aorta were selected and measured, and then, the average perimeter was calculated and recorded. The abdominal aorta with perimeter increases equalled or greater than 50% of average perimeter of mice in control was considered AAA formation. The hearts of mice were also collected and weighed.

2.5. Identification of Macrophage by Immunohistochemistry Staining. The paraffin slices of the abdominal aortic sections (4 μm thick) were examined for macrophage infiltration by immunohistochemistry staining with the monoclonal CD68 antibody (MA5-16674, Invitrogen) against mouse macrophage according to the streptavidin-peroxidase (SP) method. Brown or dark brown staining in cytoplasm was defined as positive expression. The extensity of macrophage infiltration within the abdominal aorta was quantified with Image-Pro Plus (IPP) 6.0 software by the number of positively stained cells per 0.01 mm^2 . For each animal, two slices of stained abdominal aortic sections were selected and the average number of positive cells was recorded by an investigator who was unaware of sample's identity.

2.6. Measurement of Circulating Interleukin-6 (IL-6) Levels. The peripheral blood sample was collected from mouse tail at Day 1 and Day 43. After 20-minute centrifugation, serum samples were obtained and stored at -80°C until analysis. The circulating IL-6 levels were detected with Avidin-Biotin complex (ABC)-ELISA by commercially available ELISA kit (M6000B, R&D). Testing was performed independently by a researcher who was unaware of sample's identity.

2.7. Statistical Analysis. Exploratory data analysis and Shapiro-Wilk tests were performed to determine the normality of the data distribution. Continuous variables are expressed as mean \pm SD unless otherwise noted. The self differences analyzed by paired-*t* test; differences among groups were analyzed by one-way ANOVA, followed by Dunnett's T3 test. For the incidence of AAA, counts and percentages are presented. Differences among groups were analyzed by Fisher's exact test, followed by the Bonferroni test. The relationship of two independent normality quantitative samples was analyzed by linear correlation. All analyses were conducted with statistical SPSS software 25.0 (IBM Corp., Armonk, NY, USA). The level of significant difference was set as a 2-sided $P < 0.05$.

2.8. Screening Active Compounds and Corresponding Targets. The compounds of SMYAD were screened out from the Traditional Chinese Medicine Systems Pharmacology

Database and Analysis Platform (TCMSP) database (<https://tcmsp-e.com/,Ver.2.3>) [19]. Then, the assessment of absorption, distribution, metabolism, and excretion (ADME) was employed to select active compounds that contribute to its therapeutic effects, while those with bad drug ability compounds were removed. In order to obtain compounds with higher oral absorption and utilization, the active compounds were required to meet two of the following parameters: (1) oral bioavailability (OB) equal to or greater than 30% and (2) drug likeness (DL) equal to or greater than 0.18. The canonical smiles and PubChem ID of the above active compounds were calibrated using PubChem (<https://pubchem.ncbi.nlm.nih.gov/>) [20]. Then, the corresponding target proteins with the area under curve (AUC) equal to or greater than 0.75 and possibility equal to or greater than 0.50 were obtained from TargetNet (<https://targetnet.scbdd.com>) [21]. Finally, the target proteins of SMYAD reviewed in humans were transformed into gene symbols by the UniProt database (<https://www.uniprot.org>) [22].

2.9. Construction of Network of "Compounds-Targets". Excel files containing the information of SMYAD-matched targets were established. Next, they were imported into Cytoscape 3.7.2 software [23]. Finally, the "compounds-targets" network was constructed and visualized by Cytoscape.

2.10. Collection of AAA-Related Targets. "Abdominal aortic aneurysm" and "aortic aneurysm" were selected and set as searching keywords, and then, AAA-related targets were respectively screened from four sources: (1) GeneCards database (<https://www.genecards.org/>) [24] with relevance score equal to or greater than 7.14; (2) CTD database (<https://ctdbase.org/>) [25] with inference score equal to or greater than 16.5; (3) DisGeNET database (<https://www.disgenet.org/home/>) [26] with a score equal to or greater than 0.02; and (4) OMIM database (<https://www.omim.org/geneMap>) [27]. Then, all AAA-related targets were amalgamated. Only "*Homo sapiens*" targets linked to AAA were selected and verified by their unique UniProtKB ID and target names in the UniProt database.

2.11. Screening the Common Targets of Drug and Disease. The SMYAD-matched targets and AAA-related targets were imported into the Bioinformatics platform (<https://www.bioinformatics.com.cn/>) to obtain a Venn diagram.

2.12. Enrichment Analysis. Two parts were included in enrichment analysis: Gene Ontology (GO) functional enrichment [28] and Kyoto Encyclopedia of Genes and Genomes (KEGG) pathway enrichment [29]. Then, the common targets of SMYAD and AAA were imported into the "Multiple Gene List" and implemented "Custom Analysis" in Metascape platform (<https://metascape.org>) [30]. The GO functional enrichment analysis includes biological process (BP), molecular function (MF), and cellular component (CC). Then, the enrichment analyses were

carried out with criteria as $\text{Min.Overlap} = 3$, P value cutoff = 0.01, and $\text{Min. enrichment} = 1.5$. The entries of GO were chosen and listed. The BP and KEGG pathways were selected out and visualized by Cytoscape.

2.13. Protein-Protein Interaction (PPI) Network Construction and Hub Target Screening. PPI network provides information regarding the predicted and experimental interactions of proteins. The STRING database (<https://www.string-db.org>) [31] was utilized to perform analysis with the condition of min required interaction score >0.40 . Then, the obtained PPI network was visualized by Cytoscape. Finally, the hub targets in the network were identified and ranked according to Maximal Clique Centrality (MCC) by CytoHubba algorithms [32].

2.14. Molecular Docking Verification. The 3D chemical structural formulas of chosen compounds were obtained from PubChem and energy minimizing employed to ChemBioDraw 3D. The crystal structures of selected targets were collected from the protein data bank (PDB) (<https://www.rcsb.org>) [33] for molecular docking. According to the results, the bioinformatics platform was used to draw a heat map and clustering analysis. The platform used a green, black, and red tricolor in a 100-color mode. The platform sorted the rows and columns based on the hierarchical clustering result. Then, colors were assigned to represent the binding affinity. The image was processed and visualized with a condition of scale direction (Z -score)—row, clustering direction—bidirectional, clustering method—complete, and distance method—correlation. Moreover, the binding affinity, sites, and interactions between active compounds and potential targets were achieved and analyzed by classical molecular dynamics using Auto Dock Tools-1.5.6, Pymol 2.3, and Discovery Studio 4.5 Client.

3. Results

3.1. SMYAD Inhibited Bap/Ang II-Induced AAA Formation in Mice. The timeline of Bap-/Ang II-treated AAA model and SMYAD treatment is shown in Figure 1(a). During the experimental period, no mice died accidentally. Moreover, the excretion and behavior of mice received SMYAD-low dose and SMYAD-high dose were both normal. And the weights of mice in four groups were similar at Day 1 and Day 43 (Supplementary Materials Table S1). Abdominal aorta of each animal was isolated and examined for morphological evaluation. Representative photomicrographs of each group were shown in Figure 1(b). Quantifications of morphological changes of abdominal aortas in four groups are shown in Figures 1(c) and 1(d). The perimeter of abdominal aorta was significantly increased in Bap + Ang II ($1373 \pm 113 \mu\text{m}$) than that in control ($872 \pm 31 \mu\text{m}$), which indicated the successful establishment of the AAA model. The perimeter of abdominal aorta was significantly decreased, in both Bap + Ang II + SL ($1251 \pm 93 \mu\text{m}$) and Bap + Ang II + SH ($1208 \pm 114 \mu\text{m}$), compared to Bap + Ang II. Similarly, in comparison with control (0/6), the incidence of AAA was

significantly increased to 66.7% (8/12) in Bap + Ang II ($P < 0.05$). The incidence of AAA was presented at 25.0% (3/12) and 16.7% (2/12) in Bap + Ang II + SL and Bap + Ang II + SH, respectively, which was significantly decreased compared to Bap + Ang II. Meanwhile, there was no significant difference in these indexes between Bap + Ang II + SL and Bap + Ang II + SH.

3.2. SMYAD Alleviated the Damage to Elastin Lamella Induced by Bap and Ang II. HE staining was used to evaluate the histological structure of abdominal aorta, especially for elastic lamella. Elastic lamella was known to closely related to the stability of vascular structure [34]. As shown in Figure 1(e), a representative image of HE-stained Bap + Ang II showed severe damage to vascular structure, disarray, and degradation of elastic lamella. Administrations of SMYAD could partly reverse the detrimental effects of Bap/Ang II on the elastin lamella, thereby inhibiting pathologic dilation of abdominal aorta and reducing the incidence of AAA. Furthermore, the continuity and integrity of elastin lamella in Bap + Ang II + SH was better than those in Bap + Ang II + SL.

3.3. SMYAD Mitigated Macrophage Infiltration into the Abdominal Aorta. Vascular macrophage infiltration was a clear inflammatory response, which contributed to the development of AAA and was a key event in AAA. Macrophages within the abdominal aorta were detected by immunohistochemistry staining (Figure 2(a)). The extensity of macrophage infiltration was quantified by counting the positively stained cells per 0.01 mm^2 (Figure 2(b)). The results showed the extensity of macrophage infiltration was significantly aggravated in Bap + Ang II (50 ± 5) compared to control (11 ± 2), which indicated that Bap/Ang II-induced AAA was accompanied by numerous infiltrations of macrophage. And the response was significantly inhibited by either SMYAD-low dose (23 ± 3) or SMYAD-high dose (21 ± 3). The extensity of macrophage infiltration in Bap + Ang II + SH was slighter than that in Bap + Ang II + SL, but the difference was not significant.

3.4. SMYAD Decreased Circulating Inflammation Mediator Levels. IL-6 was a clear and important mediator of inflammation, and increased circulating concentration of IL-6 had been found in patients with AAA [35]. Therefore, the circulating IL-6 levels were measured to observe the anti-inflammation effect of SMYAD on Bap-/Ang II-treated mice. As shown in Figure 2(c), there was a high positive correlation between circulating IL-6 levels and abdominal aortic perimeters ($r = 0.81$). The results shown in Figure 2(d) indicated that Bap/Ang II-induced AAA development was along with an elevated circulating IL-6 level. The circulating IL-6 level in Bap + Ang II ($78.13 \pm 13.13 \text{ pg/ml}$) was significantly increased compared to control ($22.33 \pm 1.58 \text{ pg/ml}$). And the circulating IL-6 level was significantly decreased, in both Bap + Ang II + SL ($43.75 \pm 5.29 \text{ pg/ml}$) and Bap + Ang II + SH ($44.50 \pm 5.93 \text{ pg/ml}$), compared to

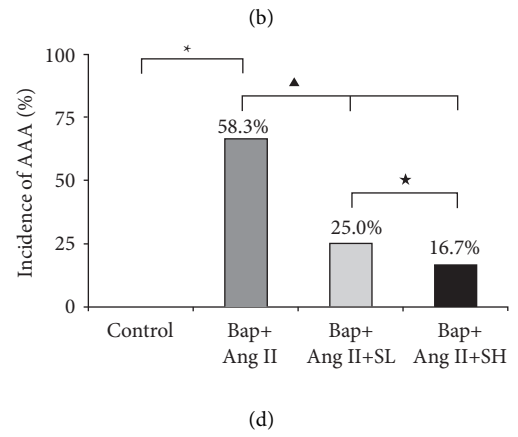
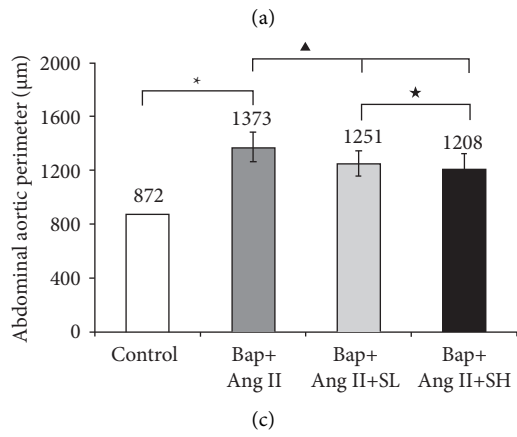
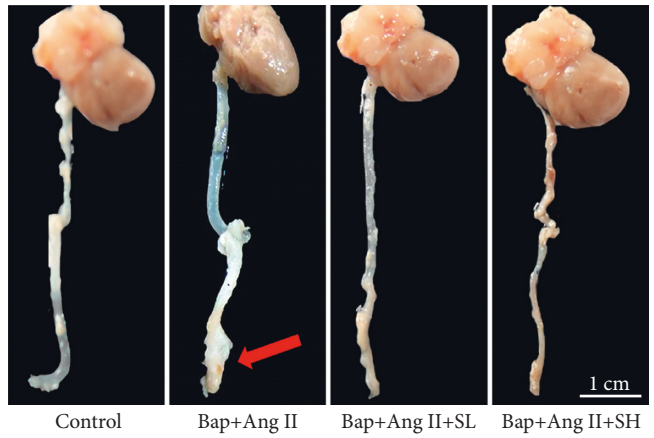
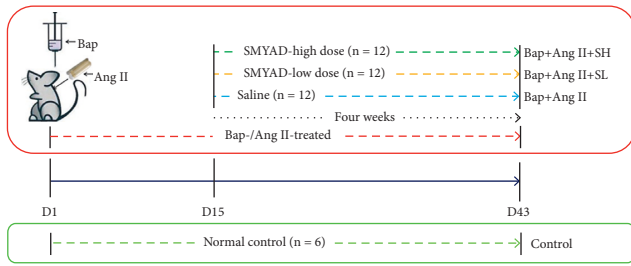


FIGURE 1: Continued.

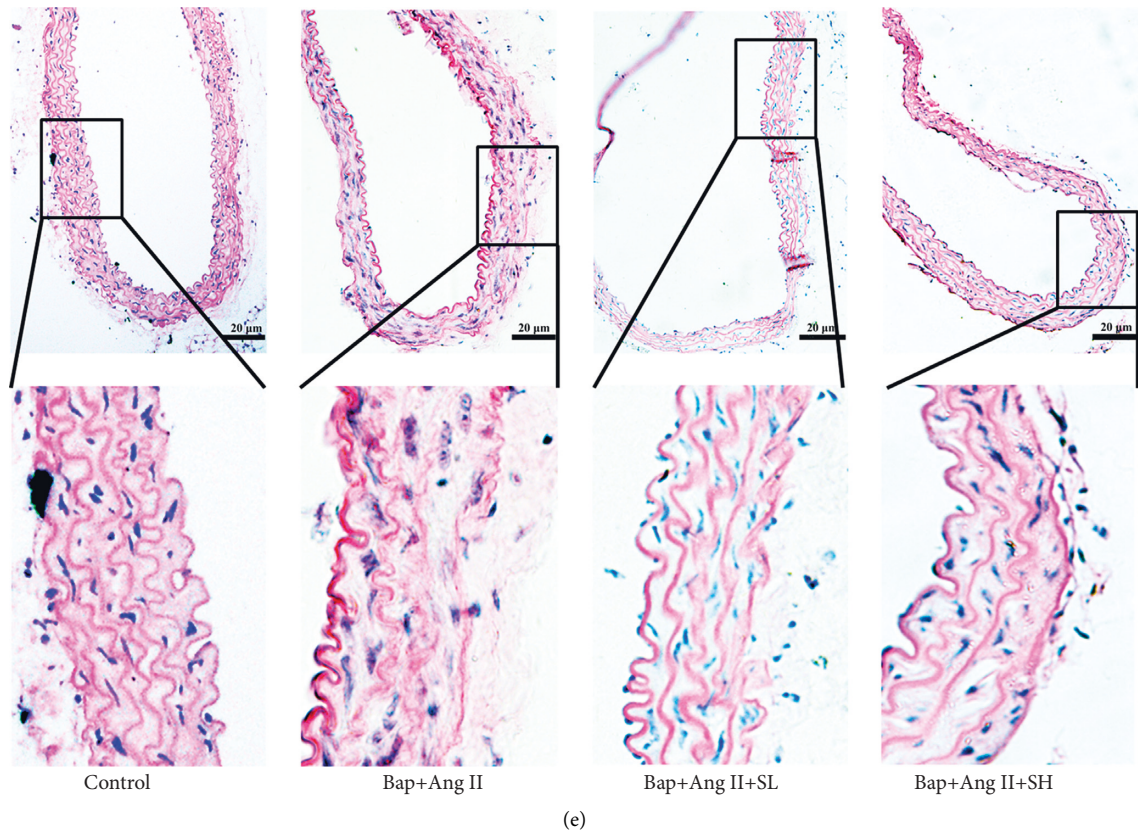


FIGURE 1: Si-Miao-Yong-An decoction (SMYAD) inhibited 3, 4-benzopyrene (Bap)/angiotensin II (Ang II)-induced AAA in mice. (a) Timeline of experimental period. (b) Representative images of abdominal aorta from normal control group (control for short), Bap-/Ang II-treated + saline group (Bap + Ang II for short), Bap-/Ang II-treated + SMYAD-low-dose group (Bap + Ang II + SL for short), and Bap-/Ang II-treated + SMYAD-high-dose group (Bap + Ang II + SH for short). No obvious pathologic expansion or hematoma formation was observed in the control. The arrow indicated pathologic expansion and abdominal aortic aneurysm (AAA) formation in Bap + Ang II. And the pathologic expansion of abdominal aortas in Bap-/Ang II-treated mice was both alleviated by SMYAD-low dose and SMYAD-high dose. (c) The perimeter of selected abdominal aortas (μm) in control ($n = 6$), Bap + Ang II ($n = 12$), Bap + Ang II + SL ($n = 12$), and Bap + Ang II + SH ($n = 12$) was measured and recorded at Day 43. Data represented the ratio or mean \pm SD. * $P < 0.05$ vs control, $\blacktriangle P < 0.05$ vs Bap + Ang II, $\star P > 0.05$ vs Bap + Ang II + SH. (d) Incidences of AAA (%) in control (0/6), Bap + Ang II (8/12), Bap + Ang II + SL (3/12), Bap + Ang II + SH (2/12). * $P < 0.05$ vs control, $\blacktriangle P < 0.05$ vs Bap + Ang II, $\star P > 0.05$ vs Bap + Ang II + SH. ((e) $\times 20$) Representative photomicrographs of abdominal aortic tissues were evaluated by using haematoxylin-eosin (HE) staining. Elastin lamella was continuous and complete in control. The elastic lamella lost fine lines and instead degraded into loosely defined lines in Bap + Ang II, and the severity of elastin lamella destruction was partly attenuated by receiving both SMYAD-low dose and SMYAD-high dose. Scale bar, 20 μm .

Bap + Ang II. There was no significant difference in circulating IL-6 levels between Bap + Ang II + SL and Bap + Ang II + SH.

3.5. Compound Screening, Target Prediction of SMYAD, and Network of "Compounds-Targets". In order to determine SMYAD-associated targets, a series of bioinformatics analyses were conducted. As shown in Table 1 and Supplementary Materials Table S2, a total of 97 active compounds of SMYAD were assayed from TCMSP and SwissADME, including 18 in *Flos Lonicerae*, 4 in *Radix Scrophulariae*, 3 in *Radix Angelica Sinensis*, and 78 in *Radix Glycyrrhizae*. Among all compounds, quercetin (C2), beta-sitosterol (C3), kaempferol (C4), and stigmasterol (C5) were the common compounds. A total of 199 SMYAD-matched targets were identified and selected from TargetNet. In order to elucidate the inner relationship between the active compounds and

SMYAD-matched targets clearly, the Cytoscape software was used to establish the "compounds-targets" network (Figure 3(a)).

3.6. AAA-Related Targets and Common Targets. A total of 1670 targets, identified from GeneCards, CTD, DisGeNET, and OMIM, were considered AAA-related targets. Then, SMYAD-matched targets and AAA-related targets were compared, 54 SMYAD-matched targets against AAA were identified (Figure 3(b)), and the common targets were subjected to further analysis.

3.7. Go and KEGG Pathway Enrichment Analysis. The 54 common targets were subjected to GO and KEGG pathway enrichment analysis to understand the potential mechanisms underlying the anti-AAA role of SMYAD. The BP

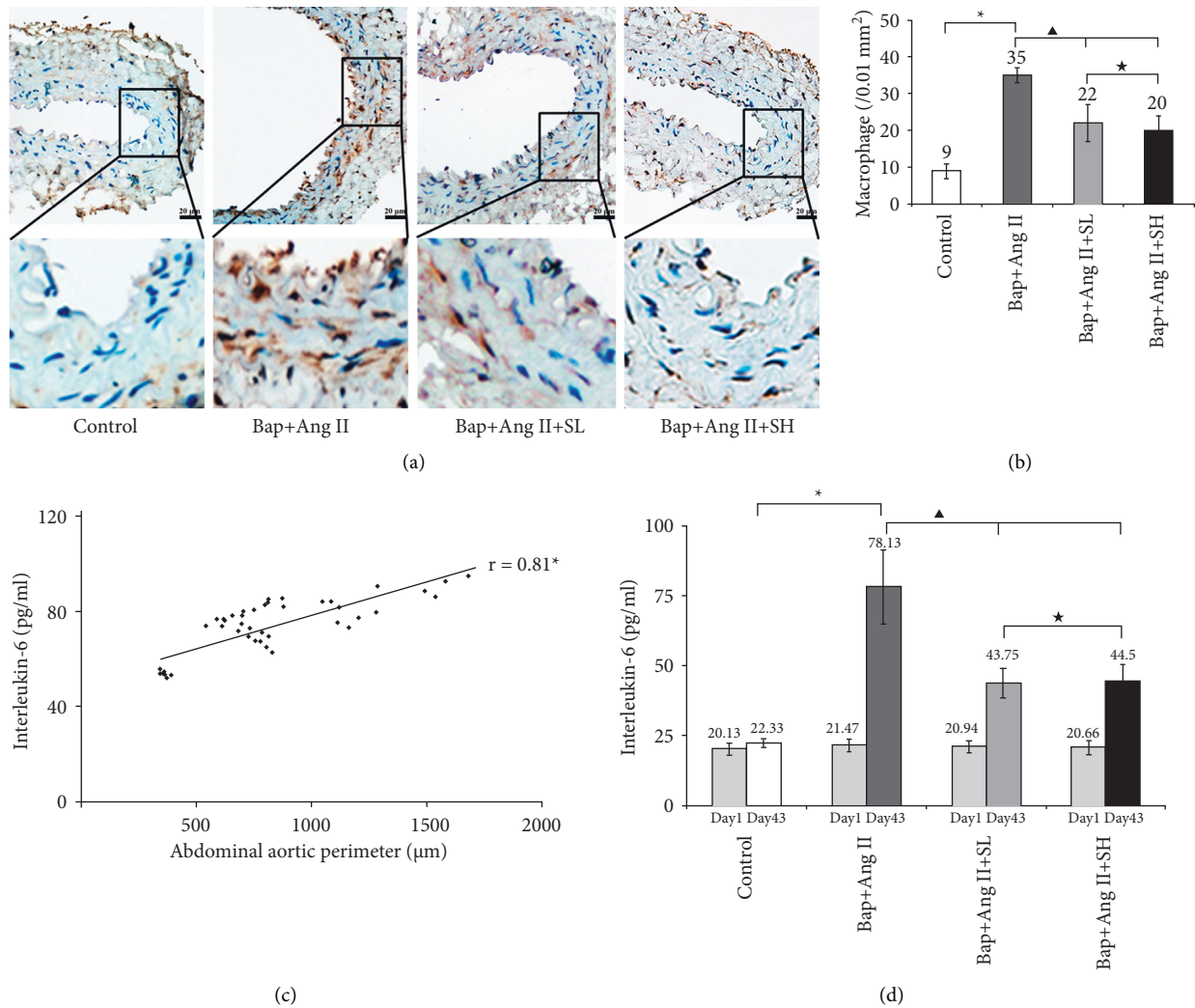


FIGURE 2: SMYAD inhibited Bap/Ang II-induced inflammatory response in mice. ((a) $\times 20$) Representative photomicrographs of immunohistochemistry staining with macrophage CD68 antibody of abdominal aortic sections from four groups. Brown or dark brown staining in cytoplasm was defined as positive expression. Scale bar 20 μm . (b) Quantification of macrophage infiltration in abdominal aortic sections. Data represented the mean \pm SD. * $P < 0.05$ vs control, $\blacktriangle P < 0.05$ vs Bap + Ang II, $\star P > 0.05$ vs Bap + Ang II + SH. (c) There was a positive correlation between circulating interleukin-6 (IL-6) levels and abdominal aortic perimeters ($r = 0.81$, $\star P < 0.05$). (d) Quantification of circulating IL-6 levels at Day 1 and Day 43. Data represented the mean \pm SD. * $P < 0.05$ vs control, $\blacktriangle P < 0.05$ vs Bap + Ang II, $\star P > 0.05$ vs Bap + Ang II + SH.

results highlighted that SMYAD modulated a series of processes related to inflammatory response, defense response, apoptotic, cell migration and adhesion, and reactive oxygen species metabolic process. In addition, there were 572 GO entries of SMYAD against AAA, including 452 BP entries, 76 MF entries, and 44 CC entries. And the top seven q -value of each GO entry is shown in Supplementary Materials Figure S1: our experimental study has revealed that SMYAD could inhibit Bap/Ang II-induced inflammation. And the KEGG pathway analysis disclosed SMYAD might regulate a series of signalling pathways related to inflammation, such as TNF signalling pathway, NF-kappa B signalling pathway, and IL-17 signalling pathway. More importantly, inflammatory responses were mediated by different classes of immune cells and mediums such as instance macrophage and interleukin, which participated

and regulated in the above signalling pathway. These findings elucidated the possible mechanisms of SMYAD against AAA and suggested that SMYAD could be a potential drug for treating AAA. Finally, the related network diagram of SMYAD-Target-BP-KEGG-AAA was established and visualized by Cytoscape software in Figure 4(a).

3.8. PPI Network and Hub Targets. Integrated network analysis to explore the hub targets regulated by SMYAD against AAA. The common targets of SMYAD and AAA were subjected to PPI interaction network analysis. Although IL-6 and TNF were the low degree value nodes in the C-T network, they were the top two highest degree value targets in the PPI network (Figure 4(b)). According to CytoHubba algorithms, top six targets in MCC score,

TABLE 1: The major active compounds of Si-Miao-Yong-An decoction.

Compound number	Name	PubChem CID	Molecular formula	MW
<i>Flos Lonicerae (Jin-Yin-Hua)</i>				
C1	Luteolin	5280445	C ₁₅ H ₁₀ O ₆	286.24
C2	Quercetin	5280343	C ₁₅ H ₁₀ O ₇	302.23
C3	Beta-sitosterol	86821	C ₂₉ H ₅₀ O	414.7
C4	Kaempferol	5280863	C ₁₅ H ₁₀ O ₆	286.24
C5	Stigmasterol	5280794	C ₂₉ H ₄₈ O	412.7
C6	Mandenol	5282184	C ₂₀ H ₃₆ O ₂	308.5
C7	Ethyl linoleate	11001	C ₂₀ H ₃₆ O ₂	308.5
C8	Phytofluenes	94171	C ₄₀ H ₆₂	542.9
C9	Beta-carotene	573	C ₄₀ H ₅₆	536.9
C10	Flavanone	10251	C ₁₅ H ₁₂ O ₂	224.25
C11	8-Indolizine carboxylic acid	11106605	C ₁₁ H ₁₅ NO ₃	209.24
C12	Chrysoeriol	5280666	C ₁₆ H ₁₂ O ₆	300.26
C13	Cryptoxanthin	182237	C ₄₀ H ₅₆ O	552.9
C14	Rhodoxanthin	92741	C ₄₀ H ₅₀ O ₂	562.8
C15	Chlorogenic acid	1794427	C ₁₆ H ₁₈ O ₉	354.3
C16	Epi-Vogeloside	14192588	C ₁₇ H ₂₄ O ₁₀	388.4
C17	Xylostosidine	4333465	C ₁₈ H ₂₅ NO ₈ S	415.5
C18	Corymbosin	10970376	C ₁₉ H ₁₈ O ₇	358.3
<i>Radix Scrophulariae (Xuan-Shen)</i>				
C3	Beta-sitostero	86821	C ₂₉ H ₅₀ O	414.7
C19	Methyl benzoate	11973336	C ₁₇ H ₁₈ O ₆	318.32
C20	Sugiol	275529	C ₂₀ H ₂₈ O ₂	300.4
C21	Harpagoside	5281542	C ₂₄ H ₃₀ O ₁₁	494.5
<i>Radix Angelicae Sinensis (Dang-Gui)</i>				
C3	Beta-sitosterol	86821	C ₂₉ H ₅₀ O	414.7
C5	Stigmasterol	5280794	C ₂₉ H ₄₈ O	412.7
C22	Ferulic acid	445858	C ₁₀ H ₁₀ O ₄	194.2

Seventy-eight compounds of *Radix Glycyrrhizin* (Gan-Cao) are shown in Supplementary File 2.

namely, IL-6, TNF, RELA, PTGS2, MMP9, and HSP90AA1, were reserved as the hub targets of SMYAD against AAA (Figure 4(c)).

3.9. Molecular Docking. Molecular docking algorithms execute quantitative predictions of binding ability, providing rankings of docked compounds-core targets based on the binding affinity. The targets, acquired from CytoHubba algorithms and literatures' supplement (NOS2, NOS3, ICAM1, PLA2G2A, SERPINE, and ESR1) [36–39], were regarded as core targets of SMYAD for treating AAA. And the corresponding proteins of these core targets were selected as receptors.

Similarly, C1-C22 compounds of SMYAD were chosen as ligands. A total of 264 times were docked, and the total binding energy of each receptor and ligand was (Figures 5(a) and 5(b)). According to the docking results, the compounds such as C15 (chlorogenic acid), C1 (luteolin), C2 (quercetin), C13 (cryptoxanthin), C10 (flavanone), C4 (kaempferol), C21 (harpagoside), and C14 (rhodoxanthin) play an important role in the treatment of AAA. Moreover, C15 had the lowest binding energy revealing that it probably be the most active compound in SMYAD; meanwhile, MMP9 had the lowest binding energy indicating that SMYAD was most likely to bind it and function as an AAA repressor. The differences of binding energy of each receptor with 22 ligands are shown in heat map (Figure 5(c)); the combination of IL-6 and C15 had

the more obvious difference in binding energy than the other types. Furthermore, the docking process was performed to concretely describe the binding sites of SMYAD against AAA. Macrophage and IL-6 were verified to be involved in the development of AAA in our experimental study; in addition, RELA was implicated in the migration and infiltration of macrophages in AAA formation [40, 41]. Among the combinations of IL-6 and RELA with C1-C22, IL-6-C15 (chlorogenic acid) and RELA-C22 (ferulic acid) had the lowest binding energy. Thus, the above combinations were docked to explore the putative conformations. The most affinity binding conformation and the corresponding intermolecular interactions were identified. The results suggested that a hydrogen bond formed between chlorogenic acid and 4NI7 on ARG-246 (3.3 Å) (Figure 5(d)). Moreover, hydrogen bonds formed between ferulic acid and 1NFlnARG-143 (3.2 Å), ARG-201 (2.9 Å), ASN-182 (3.1 Å), and ASN-200 (3.0 Å) (Figure 5(e)).

4. Discussion

In the present study, SMYAD reduced the pathological dilation of abdominal aorta and the incidence of AAA in Bap-/Ang II-treated mice. Decreased AAA formation occurred concomitantly with a reduction of elastin fiber destruction, macrophage infiltration, and expression of IL-6. These above results clearly demonstrated that SMYAD alleviated over-activated inflammation and ameliorated the

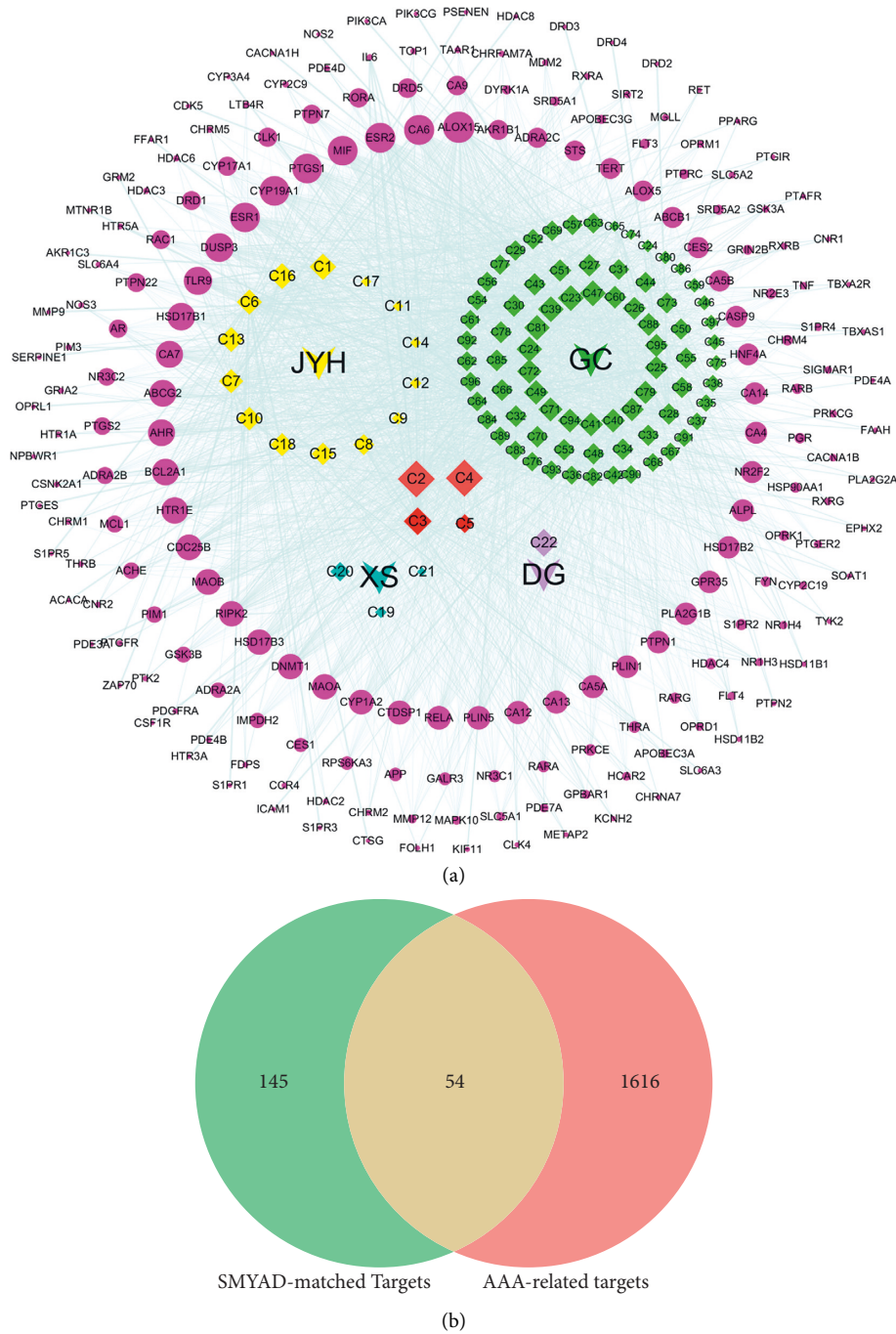


FIGURE 3: Compounds-target network and Venn diagram of SMYAD-matched and AAA-related targets of SMYAD and AAA. (a) The network of 97 active compounds from SMYAD and 199 SMYAD-matched targets (sorted by nodes degree). The rose-red ellipse nodes represented target genes. The diamond nodes represented compounds (yellow for *Flos Lonicerae*, JYH for short; blue for *Radix Scrophulariae*, XS for short; purple for *Radix Angelicae Sinensis*, DG for short; green for *Radix Glycyrrhizae*, GC for short). C2, C4 were the common compounds of JYH and GC; C3 was the common compound of JYH, XS, DG, and GC; C5 was the common compound of JYH and XS. Among all active compounds, C2, C4 were the highest degree value nodes. (b) The Venn diagram of 199 SMYAD-matched and 1670 AAA-related targets.

damage to abdominal aortic. Thus, SMYAD was a potentially protective agent for Bap/Ang II-induced AAA.

Smoking has long been considered a key risk factor for AAA. Bap, one of the major components of cigarettes, has been verified to contribute to AAA development. Furthermore, Bap

could work synergistically with Ang II to induce AAA formation in mice by promoting macrophage infiltration and disruption of elastic lamella [35]. Bap/Ang II-induced damage to the abdominal aortic more accurate delineated the pathological mechanisms of AAA development.

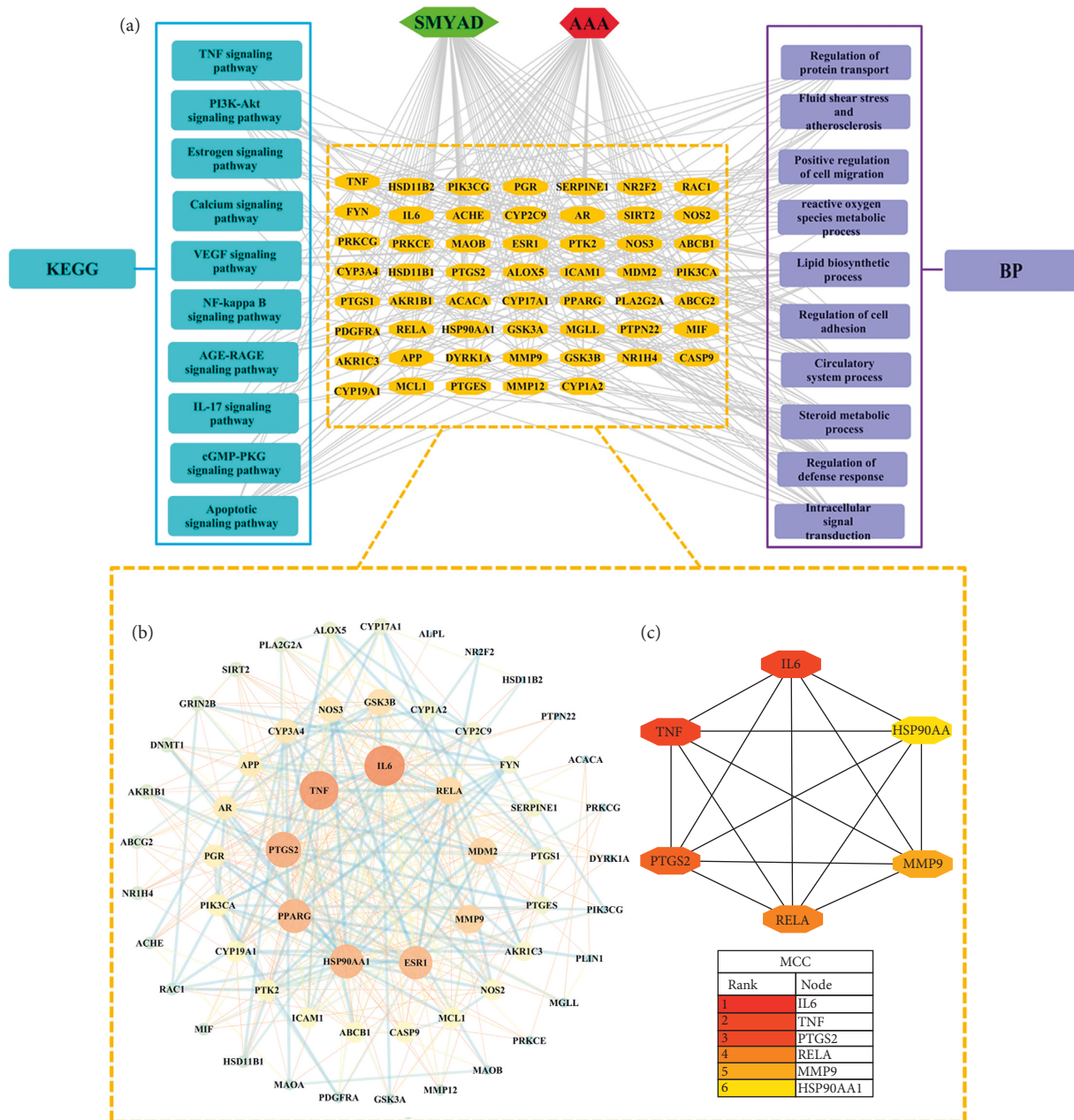
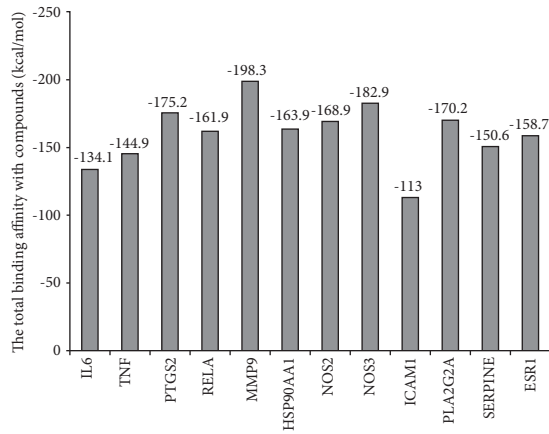


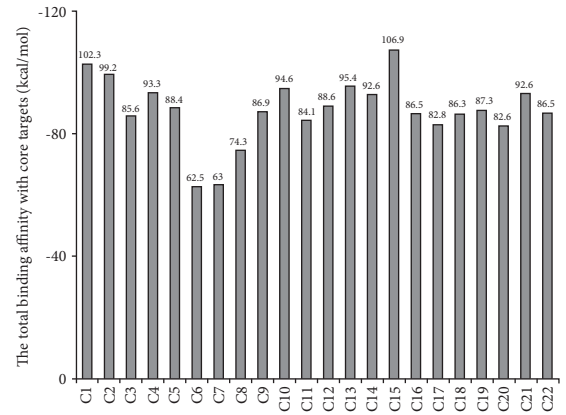
FIGURE 4: Network pharmacology-based elucidations of mechanisms of SMYAD on AAA. (a) Interaction network of SMYAD-target-biological process (BP)-Kyoto Encyclopedia of Genes and Genomes (KEGG)-AAA. The orange nodes represented the common targets of SYMAD and AAA, and the enriched BP and KEGG pathways related to inflammation and elastin lamella were selected out of top 20 q -value entries. (b) Protein-protein interaction (PPI) network was generated from string database and visualized by Cytoscape (sorted by nodes degree and edges combined score). (c) PPI network was analyzed by the CytoHubb algorithms, and the top six targets in MCC score were identified as hub targets of SMYAD against AAA.

An emerging concept is that AAA development is due to the inflammatory response, whereby many inflammatory cells and mediators have played important roles in regulating the activation of matrix-degrading proteins and smooth muscle cell apoptosis, resulting in the loss of medial elastic lamella and thinning of the tunica media [42, 43]. The pathological process of AAA starts with the infiltration and accumulation of inflammatory cells in the arterial wall [44, 45]. As the disease progresses, the inflammation in the arterial wall worsens [46]. Additionally, other inflammatory

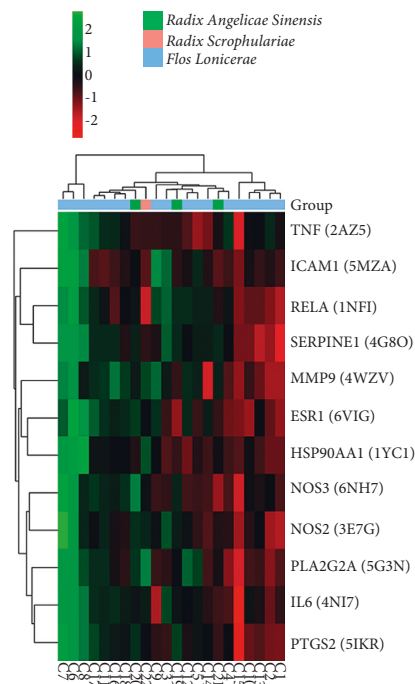
cells such as *T* and *B* cells are observed in AAA tissue samples and might play roles in AAA. Moreover, the migration and infiltration of macrophage may play a prominent role in the development of AAA [47–49]. Therefore, targeting macrophage-mediated vascular inflammation may be a potential treatment for the prevention of AAA. SMYAD has been verified to suppress the differentiation and activity of macrophage in mice [50]. Meanwhile, several studies have provided evidences that SMYAD contains multiple bioactivity effects, including anti-inflammatory, antioxidant, and



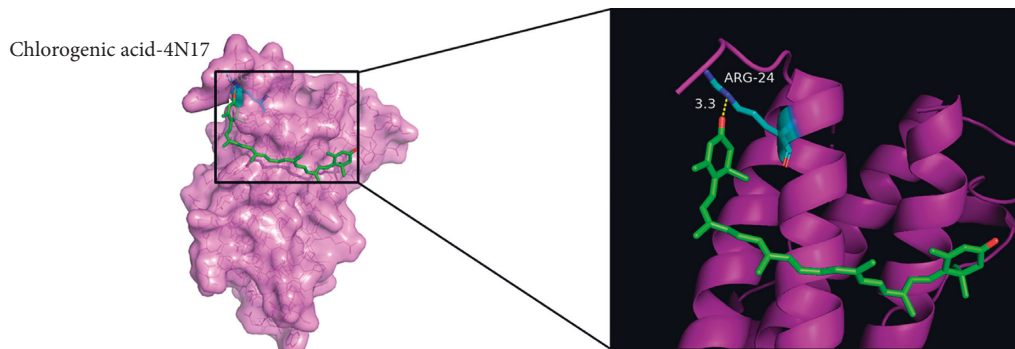
(a)



(b)



(c)



(d)

FIGURE 5: Continued.

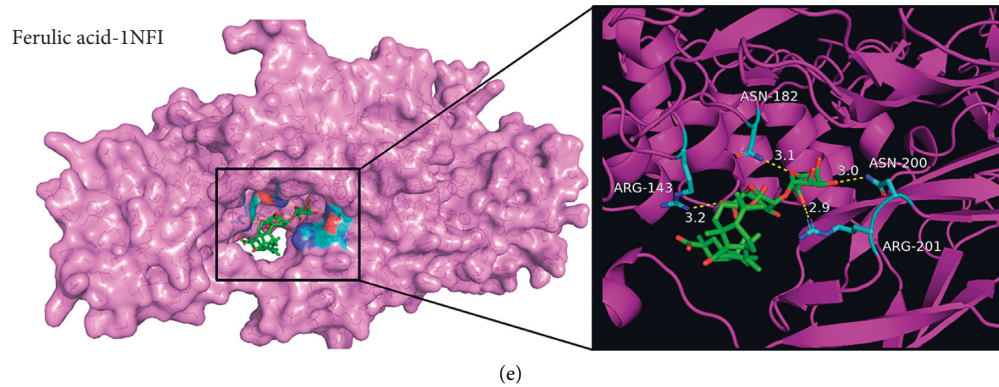


FIGURE 5: The molecular docking and sketch maps of active compounds binding to corresponding proteins of core targets. (a) The total binding energy of 12 core targets (receptors) and 22 compounds (ligands). (b) The transverse axis represented the 22 ligands; the longitudinal axis represented 12 receptors (with PDB ID). The color changed from green to red in the row represents the relative incensement of binding affinity; the combination of IL-6 and C15 had the more obvious difference in binding energy than other types. (c and d) The three-dimensional structure sites of the compounds and proteins are shown in the partial enlarged drawings. The protein backbone is represented as a cartoon. The compounds (carbon in green) and active site residues (carbon in blue) are shown in stick representation. The oxygen atom is shown as a red stick and hydrogen bonds are indicated as yellow dashed lines. (c) Site of chlorogenic acid with IL-6 (PDB ID 4NI7) and hydrogen bond formed between chlorogenic acid and 4NI7 of IL-6 on ARG-24 (3.3 Å). (d) Sites of ferulic acid with RELA (PDB ID 1NFI) and hydrogen bonds formed between ferulic acid and 1NFI protein of RELA on ARG-143 (3.2 Å), ARG-201 (2.9 Å), ASN-182 (3.1 Å), and ASN-200 (3.0 Å).

regulation of platelet activation [51–54], which are closely related to the pathogenesis of AAA. Therefore, SMYAD was supposed to have intervention effects on AAA.

Our experimental study results suggested that SMYAD has a protective effect on the deterioration of AAA. We propose the pharmacological effects of SMYAD are as follows: Firstly, SMYAD contains anti-inflammatory factors. Besides quercetin, kaempferol, and beta-sitosterol, SMYAD also contains glycyrrhizin, which is well known for its anti-inflammatory activity [55]. These potent anti-inflammatory compounds could work synergistically to suppress macrophage infiltration, to alleviate inflammation-related destruction of elastin fiber. Then, SMYAD can decrease circulating levels of IL-6. As a main pro-inflammatory cytokine, IL-6 is a pleiotropic cytokine with roles in immunity and metabolism [56], and the excessive synthesis of IL-6 and dysregulation of IL-6 receptor signalling is involved in the pathological process of AAA [57]. AAA patients have significantly higher levels of serum IL-6 than either coronary heart disease patients or control subjects [58]. Signalling via IL-6 is a causal pathway in AAA [59, 60]. Recent studies have revealed that the blockade of IL-6 had a positive outcome on disease pathology, suggesting a novel strategy for therapeutic intervention [61–63]. In Bap-/Ang II-treated mice, elevated serum IL-6 was observed, and it was specifically inhibited by SMYAD, supporting the hypothesis that IL-6 plays an important role in AAA development in patients. In addition, there is a close relationship between IL-6 and macrophage in AAA [64]. These above results suggest that SMYAD suppressed macrophage activation and IL-6 expression and thus alleviated vascular inflammation and elastin lamella disruption during AAA development. Moreover, the results from the experiment were further validated in the next following bioinformatics prediction.

Next, the network pharmacology was performed to predict the active compounds, related pathways, and core targets involved in the SMYAD-provided protection on AAA. The enrichment results disclose the pivotal participation of inflammatory response, defense response, apoptotic, cell migration and adhesion, and reactive oxygen species metabolic in the SMYAD against AAA, as well as the collaborative involvement of the TNF signalling pathway, NF-kappa B signalling pathway, PI3K-Akt signalling pathway, and IL-17 signalling pathway [65–69]. Moreover, among those common targets obtained from PPI network, the first six hub targets with higher MCC were IL-6, TNF, RELA, PTGS2, MMP9, and HSP90AA1, and they all participate in regulating the processes of inflammatory reaction [70–73]. Therefore, inflammation and subsequent destruction of elastin lamella are crucially taken part in the development of AAA. Additionally, molecular docking further illuminated the effect of SMYAD against AAA lay in the good affinity and clear binding sites between the active compounds in SMYAD and the core targets in AAA formation. IL-6, as the most important core target in the PPI network and validated objective indicator in the experimental study, has better binding ability with chlorogenic acid than with other compounds. These findings point out the direction for the SMYAD purification and further study.

There are some limitations in our study: first, the intervention dosage of SMYAD was not reasonable enough, which leads to the effect of SMYAD high-dose group, was not better than that of the SMYAD-low-dose group. So, setting another drug such as statins may better reflect the effect of SMYAD. Second, we only test for the levels of IL-6 in circulating blood, not in the tissues of abdominal aortic, making it impossible to compare the differences of IL-6 in different tissues and get more information. Third, except for

pathogenic target-IL-6, we do not know for sure whether there are protective targets in those core targets. Next, we intend to design a clinical study that focuses on the effect of SMYAD in AAA patients and screen for differential genes, to further clarify the mechanism of action.

5. Conclusions

Taken together, the experimental results and bioinformatics findings highlight the protective effect of SMYAD on AAA. Furthermore, SMYAD may be used in clinical to treat AAA, based on the identified pharmacological functions and clear signalling pathways. Moreover, the potent compounds of SMYAD against AAA were identified, supporting it as an effective medicine with clear targets for action. Thus, it may be a safe and promising drug candidate for AAA.

Data Availability

The datasets used during the present study are available from the corresponding author upon reasonable request.

Ethical Approval

The study was conducted according to the guidelines of the Declaration of Helsinki and approved by the Animal Research Ethics Committee of Wenzhou Medical University (Animal Research Qualification: X1701479).

Conflicts of Interest

The authors declare that they have no conflicts of interest.

Authors' Contributions

Z. X. (Zhenyu Xu) and L. Z. (Lulu Zhang) conceived the study; Z. X. helped with methodology; L. Z. helped with software; K. J. (Kangting Ji) validated the study; S. W. (Shenghuang Wang) helped with resources; Z. X. and F. J. (Fengchun Jiang) did the formal analysis and curated the data; Z. X. prepared the original draft of the manuscript; Z. X. and L. Z. reviewed and edited the manuscript; K. J. and N. H. (Ning Huangfu) supervised the study; Z. X. and S.W. helped with the funding acquisition. All authors have read and agreed to the published version of the manuscript.

Acknowledgments

This study was supported by Ningbo Municipal Natural Science Foundation (No. 2018A610390) and Traditional Chinese Medicine Key Project, Administration of Traditional Chinese Medicine of Zhejiang (No. 2020ZZ018).

Supplementary Materials

Figure S1: the top seven q -values of biological process (BP) entries, molecular function (MF) entries, and cell component (CC) entries related to Si-Miao-Yong-An decoction (SMYAD) against abdominal aortic aneurysm (AAA). Table S1: the body and heart weights of mice in the experimental

study. Table S2: the active compounds of *Radix Glycyrrhizin*. Figure S2: the top seven q -values of biological process (BP) entries, molecular function (MF) entries, and cell component (CC) entries. (*Supplementary Materials*)

References

- [1] S. H. Forsdahl, K. Singh, S. Solberg, and B. K. Jacobsen, "Risk factors for abdominal aortic aneurysms: a 7-year prospective study—the Tromso study, 1994–2001," *Circulation*, vol. 119, no. 16, pp. 2202–2208, 2009.
- [2] H. Abdulameer, H. Al Taii, S. G. Al-Kindi, and R. Milner, "Epidemiology of fatal ruptured aortic aneurysms in the United States (1999–2016)," *Journal of Vascular Surgery*, vol. 69, no. 2, pp. 378–384, 2019.
- [3] T. G. Walker, S. P. Kalva, K. Yeddula et al., "Clinical practice guidelines for endovascular abdominal aortic aneurysm repair: written by the standards of practice committee for the society of interventional radiology and endorsed by the cardiovascular and interventional radiological society of Europe and the Canadian interventional radiology association," *Journal of Vascular and Interventional Radiology*, vol. 21, no. 11, pp. 1632–1655, 2010.
- [4] K. D. Dansey, R. R. B. Varkevisser, N. J. Swerdlow et al., "Epidemiology of endovascular and open repair for abdominal aortic aneurysms in the United States from 2004 to 2015 and implications for screening," *Journal of Vascular Surgery*, vol. 74, no. 2, pp. 414–424, 2021.
- [5] H. H. Eckstein, D. Bockler, I. Flessenkamper, T. Schmitz-Rixen, S. Debus, and W. Lang, "Ultrasonographic screening for the detection of abdominal aortic aneurysms," *Deutsches Arzteblatt International*, vol. 106, no. 41, pp. 657–663, 2009.
- [6] S. C. Paravastu, D. Murray, J. Ghosh, F. Serracino-Inglott, J. V. Smyth, and M. G. Walker, "Inflammatory abdominal aortic aneurysms (IAAA): past and present," *Vascular and Endovascular Surgery*, vol. 43, no. 4, pp. 360–363, 2009.
- [7] G. H. Turner, A. R. Olzinski, R. E. Bernard et al., "Assessment of macrophage infiltration in a murine model of abdominal aortic aneurysm," *Journal of Magnetic Resonance Imaging*, vol. 30, no. 2, pp. 455–460, 2009.
- [8] N. Sakalihasan, R. Limet, and O. D. Defawe, "Abdominal aortic aneurysm," *Lancet (London, England)*, vol. 365, no. 9470, pp. 1577–1589, 2005.
- [9] L. Piacentini, J. P. Werba, E. Bono et al., "Genome-wide expression profiling unveils autoimmune response signatures in the perivascular adipose tissue of abdominal aortic aneurysm," *Arteriosclerosis, Thrombosis, and Vascular Biology*, vol. 39, no. 2, pp. 237–249, 2019.
- [10] N. Sakalihasan, J. B. Michel, A. Katsargyris et al., "Abdominal aortic aneurysms," *Nature Reviews Disease Primers*, vol. 4, no. 1, p. 34, 2018.
- [11] H. Takagi, Y. Mizuno, H. Yamamoto, S. N. Goto, T. Umemoto, and A. Group, "Alice in wonderland of statin therapy for small abdominal aortic aneurysm," *International Journal of Cardiology*, vol. 166, no. 1, pp. 252–255, 2013.
- [12] J. Golledge, "Abdominal aortic aneurysm: update on pathogenesis and medical treatments," *Nature Reviews Cardiology*, vol. 16, no. 4, pp. 225–242, 2019.
- [13] H. Takagi, H. Yamamoto, K. Iwata, S. Goto, T. Umemoto, and A. Group, "Effects of statin therapy on abdominal aortic aneurysm growth: a meta-analysis and meta-regression of observational comparative studies," *European Journal of Vascular and Endovascular Surgery*, vol. 44, no. 3, pp. 287–292, 2012.

- [14] Z. Pan, H. Cui, N. Wu, and H. Zhang, "Effect of statin therapy on abdominal aortic aneurysm growth rate and mortality: a systematic review and meta-analysis," *Annals of Vascular Surgery*, vol. 67, pp. 503–510, 2020.
- [15] H. X. Zhao, Z. M. Yu, Y. Geng et al., "Exploration on origin of Simiao Yong'an decoction," *China Journal of Chinese Materia Medica*, vol. 5, pp. 1209–1212, 2020.
- [16] Y. Zhao, Y. Jiang, Y. Chen et al., "Dissection of mechanisms of Chinese medicinal formula Si-Miao-Yong-an decoction protects against cardiac hypertrophy and fibrosis in isoprenaline-induced heart failure," *Journal of Ethnopharmacology*, vol. 248, Article ID 112050, 2020.
- [17] L. Yanling and L. Dayong, "Treatment of abdominal aortic aneurysm with modified Simiao Yong'an decoction," *Journal of Modern Integrative Medicine*, vol. 16, no. 5, p. 627, 2007.
- [18] S. Keerthikumar, "An introduction to proteome bioinformatics," *Methods in Molecular Biology*, vol. 1549, pp. 1–3, 2017.
- [19] J. Ru, P. Li, J. Wang et al., "TCMSP: a database of systems pharmacology for drug discovery from herbal medicines," *Journal of Cheminformatics*, vol. 6, p. 13, 2014.
- [20] S. Kim, J. Chen, T. Cheng et al., "PubChem in 2021: new data content and improved web interfaces," *Nucleic Acids Research*, vol. 49, no. D1, pp. D1388–D1395, 2021.
- [21] Z. J. Yao, J. Dong, Y. J. Che et al., "TargetNet: a web service for predicting potential drug-target interaction profiling via multi-target SAR models," *Journal of Computer-Aided Molecular Design*, vol. 30, no. 5, pp. 413–424, 2016.
- [22] The UniProt Consortium, "UniProt: the universal protein knowledgebase in 2021," *Nucleic Acids Research*, vol. 49, no. D1, pp. D480–D489, 2021.
- [23] P. Shannon, A. Markiel, O. Ozier et al., "Cytoscape: a software environment for integrated models of biomolecular interaction networks," *Genome Research*, vol. 13, no. 11, pp. 2498–2504, 2003.
- [24] G. Stelzer, N. Rosen, I. Plaschkes et al., "The genecards suite: from gene data mining to disease genome sequence analyses," *Current Protocols in Bioinformatics*, vol. 54, pp. 1.30.31–1.30.33, 2016.
- [25] A. P. Davis, C. J. Grondin, R. J. Johnson et al., "Comparative toxicogenomics database (CTD): update 2021," *Nucleic Acids Research*, vol. 49, no. D1, pp. D1138–D1143, 2021.
- [26] J. Pinero, A. Bravo, N. Queralt-Rosinach et al., "DisGeNET: a comprehensive platform integrating information on human disease-associated genes and variants," *Nucleic Acids Research*, vol. 45, no. D1, pp. D833–D839, 2017.
- [27] J. S. Amberger, A. Hamosh, "Searching online mendelian inheritance in man (OMIM): a knowledgebase of human genes and genetic phenotypes," *Current Protocols in Bioinformatics*, vol. 58, pp. 1.2.1–1.2.12, 2017.
- [28] The Gene Ontology Consortium, "Expansion of the gene ontology knowledgebase and resources," *Nucleic Acids Research*, vol. 45, no. D1, pp. D331–D338, 2017.
- [29] M. Kanehisa, M. Furumichi, M. Tanabe, Y. Sato, and K. Morishima, "KEGG: new perspectives on genomes, pathways, diseases and drugs," *Nucleic Acids Research*, vol. 45, no. D1, pp. D353–D361, 2017.
- [30] Y. Zhou, B. Zhou, L. Pache et al., "Metascape provides a biologist-oriented resource for the analysis of systems-level datasets," *Nature Communications*, vol. 10, no. 1, p. 1523, 2019.
- [31] D. Szklarczyk, A. L. Gable, K. C. Nastou et al., "The STRING database in 2021: customizable protein-protein networks, and functional characterization of user-uploaded gene/ measurement sets," *Nucleic Acids Research*, vol. 49, no. D1, pp. D605–D612, 2021.
- [32] C.-H. Chin, S.-H. Chen, H.-H. Wu, C.-W. Ho, M.-T. Ko, and C.-Y. Lin, "cytoHubba: identifying hub objects and sub-networks from complex interactome," *BMC Systems Biology*, vol. 8, no. S4, p. S11, 2014.
- [33] S. K. Burley, H. M. Berman, G. J. Kleywegt, J. L. Markley, H. Nakamura, and S. Velankar, "Protein data bank (PDB): the single global macromolecular structure archive," *Methods in Molecular Biology*, vol. 1607, pp. 627–641, 2017.
- [34] S. Yousef, N. Matsumoto, I. Dabe et al., "Quantitative not qualitative histology differentiates aneurysmal from non-dilated ascending aortas and reveals a net gain of medial components," *Scientific Reports*, vol. 11, no. 1, p. 13185, 2021.
- [35] Y. Zhang and K. S. Ramos, "The development of abdominal aortic aneurysms in mice is enhanced by benzo (a) pyrene," *Vascular Health and Risk Management*, vol. 4, no. 5, pp. 1095–1102, 2008.
- [36] M. Toral, A. De la Fuente-Alonso, M. R. Campanero, and J. M. Redondo, "The NO signalling pathway in aortic aneurysm and dissection," *British Journal of Pharmacology*, vol. 179, pp. 1287–1303, 2022.
- [37] E. S. Liang, W. W. Bai, H. Wang et al., "Parp-1 (poly [ADP-ribose] polymerase 1) inhibition protects from ang II (angiotensin II) -induced abdominal aortic aneurysm in mice," *Hypertension*, vol. 72, no. 5, pp. 1189–1199, 2018.
- [38] H. Fraser, C. Hislop, R. M. Christie et al., "Varespladib (A-002), a secretory phospholipase A2 inhibitor, reduces atherosclerosis and aneurysm formation in ApoE^{-/-} mice," *Journal of Cardiovascular Pharmacology*, vol. 53, no. 1, pp. 60–65, 2009.
- [39] D. Flondell-Site, B. Lindblad, T. Kolbel, and A. Gottsater, "Markers of proteolysis, fibrinolysis, and coagulation in relation to size and growth rate of abdominal aortic aneurysms," *Vascular and Endovascular Surgery*, vol. 44, no. 4, pp. 262–268, 2010.
- [40] T. Mi, B. Nie, C. Zhang, and H. Zhou, "The elevated expression of osteopontin and NF-kappaB in human aortic aneurysms and its implication," *Journal of Huazhong University of Science and Technology*, vol. 31, no. 5, p. 602, 2011.
- [41] A. Watanabe, T. Ichiki, C. Sankoda et al., "Suppression of abdominal aortic aneurysm formation by inhibition of prolyl hydroxylase domain protein through attenuation of inflammation and extracellular matrix disruption," *Clinical Science*, vol. 126, no. 9, pp. 671–678, 2014.
- [42] H. Li, S. Bai, Q. Ao et al., "Modulation of immune-inflammatory responses in abdominal aortic aneurysm: emerging molecular targets," *Journal of Immunology Research*, vol. 2018, Article ID 7213760, 15 pages, 2018.
- [43] E. Arnaoutoglou, G. Kouvelos, A. Koutsoumpelis, N. Patelis, A. Lazaris, and M. Matsagkas, "An update on the inflammatory response after endovascular repair for abdominal aortic aneurysm," *Mediators of Inflammation*, vol. 2015, Article ID 945035, 6 pages, 2015.
- [44] C. M. Crawford, K. Hurtgen-Grace, E. Talarico, and J. Marley, "Abdominal aortic aneurysm: an illustrated narrative review," *Journal of Manipulative and Physiological Therapeutics*, vol. 26, no. 3, pp. 184–195, 2003.
- [45] K. Saraff, F. Babamusta, L. A. Cassis, and A. Daugherty, "Aortic dissection precedes formation of aneurysms and atherosclerosis in angiotensin II-infused, apolipoprotein E-deficient mice," *Arteriosclerosis, Thrombosis, and Vascular Biology*, vol. 23, no. 9, pp. 1621–1626, 2003.

- [46] J. P. Meekel, M. Dias-Neto, N. Bogunovic et al., "Inflammatory gene expression of human perivascular adipose tissue in abdominal aortic aneurysms," *European Journal of Vascular and Endovascular Surgery*, vol. 61, no. 6, pp. 1008–1016, 2021.
- [47] N. D. Forester, S. M. Cruickshank, D. J. Scott, and S. R. Carding, "Functional characterization of T cells in abdominal aortic aneurysms," *Immunology*, vol. 115, no. 2, pp. 262–270, 2005.
- [48] L. Canes, J. Alonso, C. Ballester-Servera et al., "Targeting tyrosine hydroxylase for abdominal aortic aneurysm: impact on inflammation, oxidative stress, and vascular remodeling," *Hypertension*, vol. 78, no. 3, pp. 681–692, 2021.
- [49] M.-T. Chiang, I.-M. Chen, F.-F. Hsu et al., "Gal-1 (galectin-1) upregulation contributes to abdominal aortic aneurysm progression by enhancing vascular inflammation," *Arteriosclerosis, Thrombosis, and Vascular Biology*, vol. 41, no. 1, pp. 331–345, 2021.
- [50] X. N. Chen, Q. H. Ge, Y. X. Zhao, X. C. Guo, and J. P. Zhang, "Effect of Si-Miao-Yong-An decoction on the differentiation of monocytes, macrophages, and regulatory T cells in ApoE (-/-) mice," *Journal of Ethnopharmacology*, vol. 276, Article ID 114178, 2021.
- [51] C. Su, Q. Wang, H. Luo et al., "Si-Miao-Yong-An decoction attenuates cardiac fibrosis via suppressing TGF-beta1 pathway and interfering with MMP-TIMPs expression," *Biomedicine & Pharmacotherapy*, vol. 127, Article ID 110132, 2020.
- [52] L. Li, X. Chen, C. Su et al., "Si-Miao-Yong-An decoction preserves cardiac function and regulates GLC/AMPK/NF-kappaB and GLC/PPARalpha/PGC-1alpha pathways in diabetic mice," *Biomedicine & Pharmacotherapy*, vol. 132, Article ID 110817, 2020.
- [53] Y. Ren, X. Chen, P. Li et al., "Si-Miao-Yong-An decoction ameliorates cardiac function through restoring the equilibrium of SOD and NOX2 in heart failure mice," *Pharmacological Research*, vol. 146, Article ID 104318, 2019.
- [54] C. Su, Q. Wang, H. Zhang et al., "Si-Miao-Yong-An decoction protects against cardiac hypertrophy and dysfunction by inhibiting platelet aggregation and activation," *Frontiers in Pharmacology*, vol. 10, p. 990, 2019.
- [55] T. C. Kao, M. H. Shyu, and G. C. Yen, "Glycyrrhizic acid and 18beta-glycyrrhetinic acid inhibit inflammation via PI3K/Akt/GSK3beta signaling and glucocorticoid receptor activation," *Journal of Agricultural and Food Chemistry*, vol. 58, no. 15, pp. 8623–8629, 2010.
- [56] S. Kang, T. Tanaka, M. Narazaki, and T. Kishimoto, "Targeting interleukin-6 signaling in clinic," *Immunity*, vol. 50, no. 4, pp. 1007–1023, 2019.
- [57] E. Paige, M. Clement, F. Lareyre et al., "Interleukin-6 receptor signaling and abdominal aortic aneurysm growth rates," *Circulation: Genomic and Precision Medicine*, vol. 12, no. 2, Article ID e002413, 2019.
- [58] S. C. Harrison, A. J. Smith, G. T. Jones et al., "Interleukin-6 receptor pathways in abdominal aortic aneurysm," *European Heart Journal*, vol. 34, no. 48, pp. 3707–3716, 2013.
- [59] L. Smallwood, R. Allcock, F. Van Bockxmeer et al., "Polymorphisms of the interleukin-6 gene promoter and abdominal aortic aneurysm," *European Journal of Vascular and Endovascular Surgery*, vol. 35, no. 1, pp. 31–36, 2008.
- [60] H. Takagi, T. Watanabe, Y. Mizuno, N. Kawai, T. Umemoto, and All-Literature Investigation of Cardiovascular Evidence Group, "Circulating interleukin-6 levels are associated with abdominal aortic aneurysm presence: a meta-analysis and meta-regression of case-control studies," *Annals of Vascular Surgery*, vol. 28, no. 8, pp. 1913–1922, 2014.
- [61] G. Schett, D. Elewaut, I. B. McInnes, J. M. Dayer, and M. F. Neurath, "How cytokine networks fuel inflammation: toward a cytokine-based disease taxonomy," *Nature Medicine*, vol. 19, no. 7, pp. 822–824, 2013.
- [62] E. H. Choy, A. F. Kavanaugh, and S. A. Jones, "The problem of choice: current biologic agents and future prospects in RA," *Nature Reviews Rheumatology*, vol. 9, no. 3, pp. 154–163, 2013.
- [63] T. Tanaka, M. Narazaki, and T. Kishimoto, "IL-6 in inflammation, immunity, and disease," *Cold Spring Harbor Perspectives in Biology*, vol. 6, no. 10, Article ID a016295, 2014.
- [64] W. Xu, Y. Chao, M. Liang, K. Huang, and C. Wang, "CTRP13 mitigates abdominal aortic aneurysm formation via NAMPT1," *Molecular Therapy*, vol. 29, no. 1, pp. 324–337, 2020.
- [65] S. Schubl, S. Tsai, E. J. Ryer et al., "Upregulation of protein kinase cdelta in vascular smooth muscle cells promotes inflammation in abdominal aortic aneurysm," *Journal of Surgical Research*, vol. 153, no. 2, pp. 181–187, 2009.
- [66] S. Morgan, D. Yamanouchi, C. Harberg et al., "Elevated protein kinase C-delta contributes to aneurysm pathogenesis through stimulation of apoptosis and inflammatory signaling," *Arteriosclerosis, Thrombosis, and Vascular Biology*, vol. 32, no. 10, pp. 2493–2502, 2012.
- [67] X.-Q. Ni, Y.-R. Zhang, L.-X. Jia et al., "Inhibition of Notch1-mediated inflammation by intermedin protects against abdominal aortic aneurysm via PI3K/Akt signaling pathway," *Aging (Albany NY)*, vol. 13, no. 4, pp. 5164–5184, 2021.
- [68] M. Romain, S. Taleb, M. Dalloz et al., "Overexpression of SOCS3 in T lymphocytes leads to impaired interleukin-17 production and severe aortic aneurysm formation in mice—brief report," *Arteriosclerosis, Thrombosis, and Vascular Biology*, vol. 33, no. 3, pp. 581–584, 2013.
- [69] J. Wang, H. Sun, Y. Zhou et al., "Circular RNA microarray expression profile in 3, 4-benzopyrene/angiotensin II-induced abdominal aortic aneurysm in mice," *Journal of Cellular Biochemistry*, vol. 120, no. 6, pp. 10484–10494, 2019.
- [70] S. Mosawy, D. E. Jackson, O. L. Woodman, and M. D. Linden, "The flavonols quercetin and 3', 4'-dihydroxyflavonol reduce platelet function and delay thrombus formation in a model of type 1 diabetes," *Diabetes and Vascular Disease Research*, vol. 11, no. 3, pp. 174–181, 2014.
- [71] J. H. Choi, S. E. Park, S. J. Kim, and S. Kim, "Kaempferol inhibits thrombosis and platelet activation," *Biochimie*, vol. 115, pp. 177–186, 2015.
- [72] T. Rajavel, P. Packiyaraj, V. Suryanarayanan, S. K. Singh, K. Ruckmani, and K. Pandima Devi, "Beta-sitosterol targets Trx/Trx1 reductase to induce apoptosis in A549 cells via ROS mediated mitochondrial dysregulation and p53 activation," *Scientific Reports*, vol. 8, no. 1, p. 2071, 2018.
- [73] J. N. Choi, Y. H. Choi, J. M. Lee et al., "Anti-inflammatory effects of beta-sitosterol-beta-D-glucoside from trachelospermum jasminoides (apocynaceae) in lipopolysaccharide-stimulated RAW 264.7 murine macrophages," *Natural Product Research*, vol. 26, no. 24, pp. 2340–2343, 2012.